

# **THERMAL PERFORMANCE OF A CRYOGENIC FLUID MANAGEMENT CUBESAT MISSION**

**J. J. Berg, J. M. Oliveira, and J. F. Congiardo**  
Analysis Branch, NASA Kennedy Space Center, FL

**L. K. Walls**  
Launch Services Program, NASA Kennedy Space Center, FL

**P. T. Putman and M. S. Haberbusch**  
Sierra Lobo Inc., OH

## **ABSTRACT**

Development for an in-space demonstration of a CubeSat as a Cryogenic Fluid Management (CFM) test bed is currently underway. The favorable economics of CubeSats make them appealing for technology development activity. While their size limits testing to smaller scales, many of the regimes relevant to CFM can still be achieved. The first demo flight of this concept, CryoCube®-1, will focus on oxygen liquefaction and low-gravity level sensing using Reduced Gravity CryoTracker®. An extensive thermal modeling effort has been underway to both demonstrate concept feasibility and drive the prototype design. The satellite will utilize both a sun- and earth-shield to passively cool its experimental tank below 115 K. An on-board gas generator will create high pressure gaseous oxygen, which will be throttled into a bottle in the experimental node and condensed. The resulting liquid will be used to perform various experiments related to level sensing. Modeling efforts have focused on the spacecraft thermal performance and its effects on condensation in the experimental node. Parametric analyses for both optimal and suboptimal conditions have been considered and are presented herein.

## **INTRODUCTION**

NASA has identified the storage and transfer of cryogenic propellants in microgravity as a primary technology development area that will be critical for future exploration efforts. (Meyer, Johnson, Palaszewski, Goebel, White, & Coote, 2012) To enable these technologies, including zero boil off, propellant acquisition, and automated transfer, a better knowledge of cryogenic fluid behavior is required. Increasing the fidelity of existing modeling techniques and flight qualifying low technology readiness level (TRL) devices requires additional experimental data.

Several flight experiments at different scales that are in various stages of development will gather data relevant to CFM. However, these experiments are limited to the use of simulant fluids or are of such budget consequence that they must limit risk and therefore restrict the types of technologies that may be tested. CryoCube-1 (CC-1) will address both of these limitations by carrying actual cryogenic propellants while maintaining the low cost and relatively liberal risk posture of the CubeSat platform.

The main technology being tested with CC-1 is the Sierra Lobo Inc. (SLI) Reduced Gravity CryoTracker®. This sensor allows for mass gauging of propellants, and is derivative of the conventional CryoTracker®. It was developed under the NASA Small Business Innovation Research program, and was tested aboard the ZERO-G airplane and has advanced to TRL 5.

CC-1 will utilize liquid oxygen as the working fluid. CubeSat requirements forbid the use of pressure vessels during launch. Therefore, oxygen will be stored in a solid state and evolved into a pressurized gas with a gas generator. Further, due to the size and power constraints inherent in a small satellite, passive radiation cooling will be utilized to reach the cryogenic temperatures necessary to liquefy the gaseous oxygen. Data will be collected with the CryoTracker® sensor and an internal camera. CC-1 will be carried to low earth orbit as a secondary payload in 2014.

A thermal analysis of the complete satellite bus and gas generator system was required to characterize system performance, drive material selection, insure sufficient thermal margins, and guide orbit selection. This analysis was performed using the software package C&R Thermal Desktop.

## **OXYGEN CONDENSATION**

The chief factor governing the feasibility of the project is whether the gaseous oxygen generated can be condensed into liquid form. This will dictate the required temperature of the experiment tank. The gas generator has the ability to generate oxygen at 473 K and up to 5 MPa. Using the software REFPROP, the pressure and temperature of hence phase of the oxygen can be known.

Complications can arise because as the gaseous oxygen is cooled, its pressure also falls. Therefore, the initial generated pressure must be high enough that after cooling, the pressure is still such that the oxygen remains in liquid phase. The effect is seen in Figure 1, which plots the pressure in the experiment tank versus the temperature of the tank walls and hence the oxygen. It is assumed that the liquid will at steady state reach a thermal equilibrium where both are essentially the same temperature.

The yellow shaded area, below the black line, shows where oxygen will remain in gaseous form. The light blue area between the red and black lines is the region in which oxygen generated at the given pressure will remain in gaseous form due to falling pressure during cooling. The dark blue region shows the pressures required so that the oxygen will condense into a liquid after cooling.

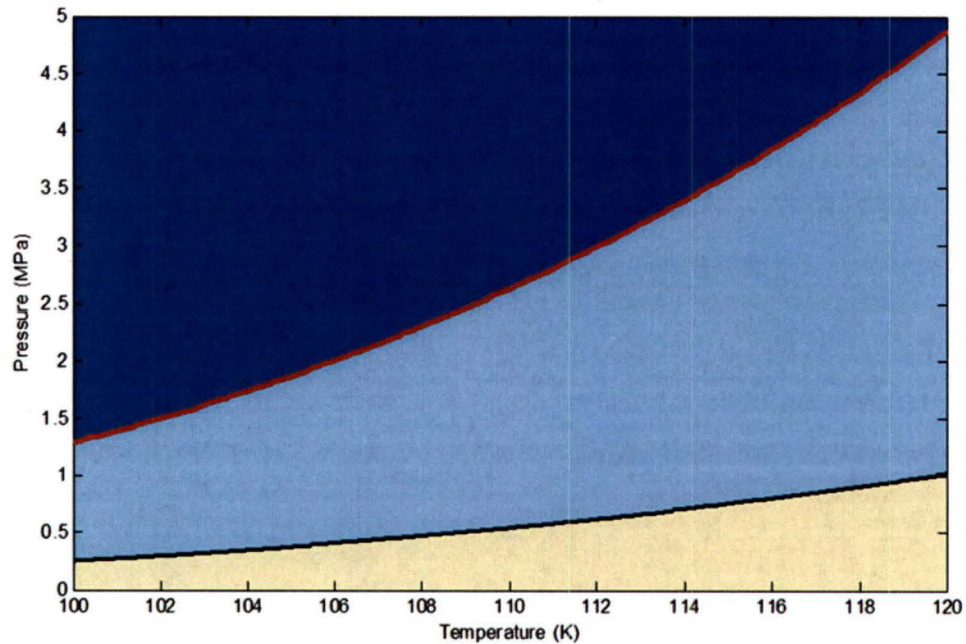


**Figure 1 – The phase plot of oxygen.**

Therefore, due to the 5 MPa maximum possible pressure, the tank wall temperature must be below 120 K.

### **SATELLITE STRUCTURE**

The CubeSat platform presents a challenging environment for maintaining low temperatures. They have limited capability for maneuver and pointing and the small size prevents having a large physical barrier between hot and cold sections of the spacecraft. CC-1 addresses these problems with radiation shields and thermal isolation between spacecraft sections with different functions.

CC-1 features two radiation shields that are constructed largely of multi-layer insulation. The first is designed to block solar radiation and also integrates the solar panels for energy collection. The second is for blocking infrared radiation from the earth. The shields operate in concert during different portions of the orbit to limit the heating load on the satellite.

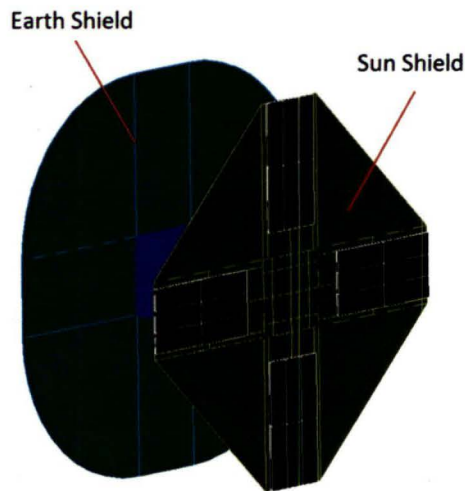


**Figure 2 – CC-1 satellite radiation shields.**

The satellite is constructed to take advantage of as many commercially available CubeSat components as feasible. The main chassis is a standard 1.5U (10x10x15 cm) 7075 aluminum skeletonized frame. Between the chassis and the experiment section is the gas generator housing. This housing is an integral part of the structure, and also serves to separate the hot and cold ends of the CubeSat. Attaching these components are thin, low thermal conductivity G-10 composite standoffs. To block radiation heat transfer, MLI barriers are placed between each section.

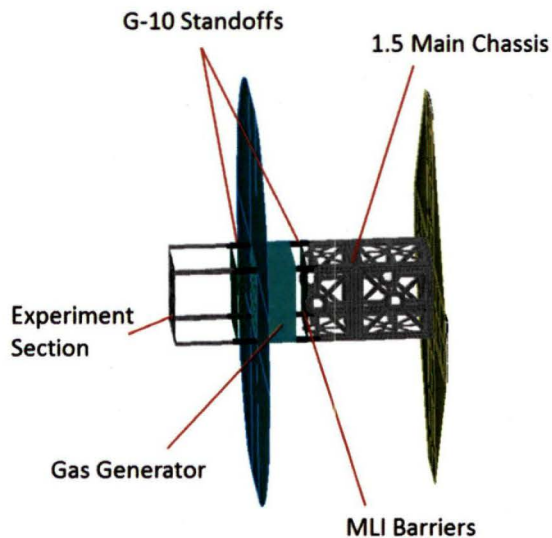


**Figure 3 – Thermal design components of the main structure.**

For fine control over the radiation that reaches the experiment tank and to maximize the tank's exposure to deep space for radiative cooling, the experiment section has actuating doors that open during certain orbital positions. The tank also features fins to increase the surface area for radiation heat exchange.

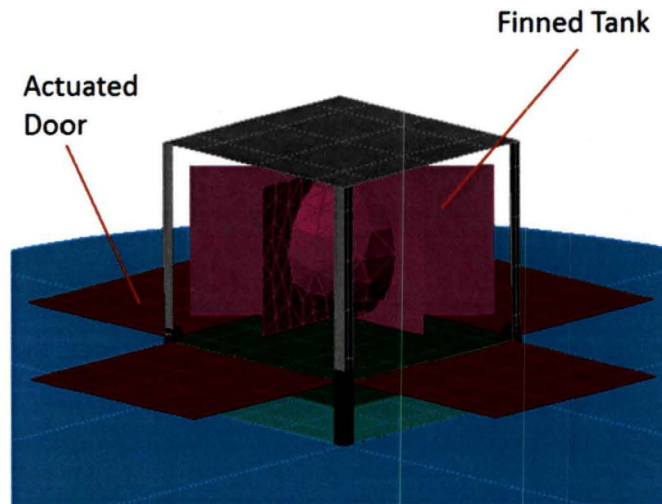


**Figure 4 – Focus on actuated doors.**

The model also features the various internal components necessary for operation. These parts include the battery, main board, processor, the camera control card, power supply, radio transmitter, and attitude control card. Appropriate heat loads were estimated for each and applied to the model.

### **RADIATION MANAGEMENT**

The pointing position of the spacecraft is controlled by magnet torquers. The attitude is adjusted to maximize the effectiveness of the radiation (sun and earth) shields on the craft. During the part of the orbit in which the craft is in the sunlight, the spacecraft will keep its long axis parallel to sun rays (sun pointing). This will allow the craft to be in complete shadow from the sun, but it will be exposed to earth IR.

When the craft moves into eclipse and sunlight is now no longer a factor, the craft repositions itself to point its long axis directly normal to the surface of the earth (nadir pointing). This allows the sun shield to partly block earth IR from bombarding the side of the craft. It also allows the earth shield to entirely block the experiment U from any earth IR. The behavior is illustrated in Figure 5.

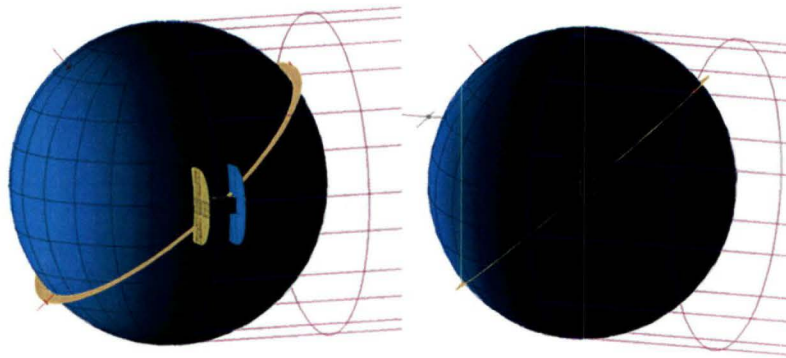


**Figure 5 – The two pointing modes for CC-1.**

The sizing of the radiation shields is critical. Due to the virtually parallel nature of the rays from the sun when in earth orbit, the sun shield on the spacecraft is adequate for blocking sunlight from the majority of the spacecraft. However, the shield is not large enough to effectively block earth IR when in earth pointing mode. Increasing the size of the sun shield is not feasible due to the angular size of earth in LEO. The geometry of the situation is shown in Figure 6.

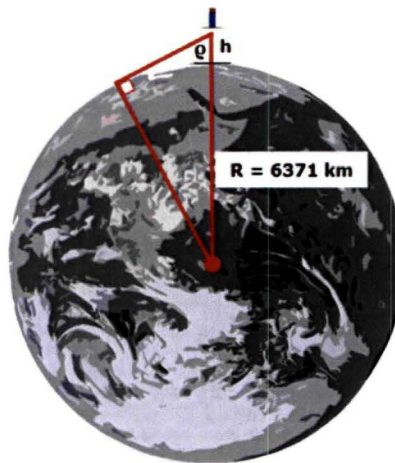


**Figure 6 – Apparent angular size of Earth in LEO.**

Using the geometry given in Figure 6 and the dimensions of the craft, the size of the shield required to block earth IR from reaching the experiment U can be determined. This is shown in Figure 7 for two different mounting locations: where the sun shield is located and where the actual earth shield is mounted between the 2U and experiment U. This explains the design choice regarding the mounting location and size of the earth shield. The maximum stowable size is derived from the length of the satellite and the avoidance of complicated double-folding shield panels.

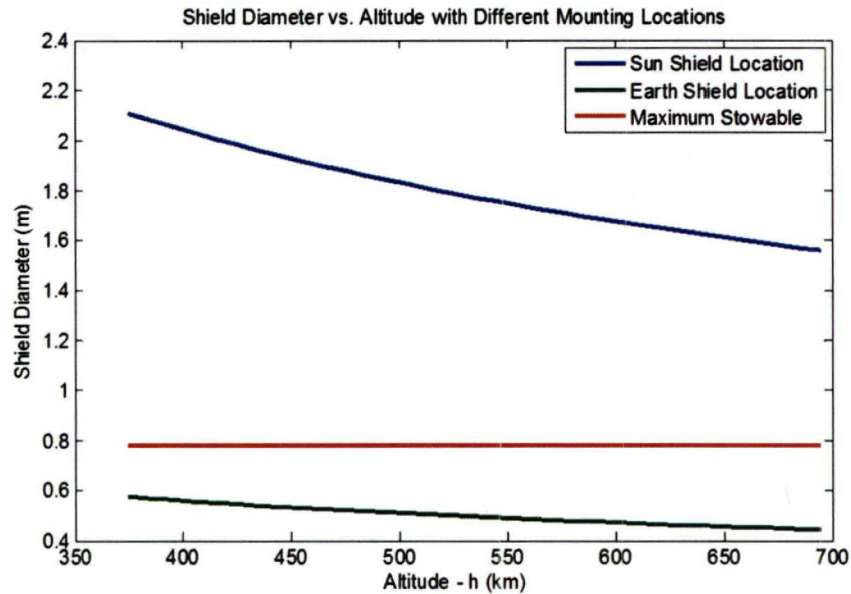


**Figure 7 – Radiation shield size determination plot.**

During eclipse, the actuated doors on the experiment U open and expose the tank to deep space. This is the only way to passively achieve low temperatures while in a low altitude orbit. When in the shade, and the satellite is in earth pointing mode, the tank should only be able to “see” the earth shield, the structure surrounding it, and deep space. The more time that can be spent with the doors open, the colder the tank will be. However, there may be portions of an orbit where a single door could be opened to provide a partial view of deep space. In this case, a trade would exist between exposure time to a radiation sink, and possible reflections of earth IR off of the shield back on to the tank.

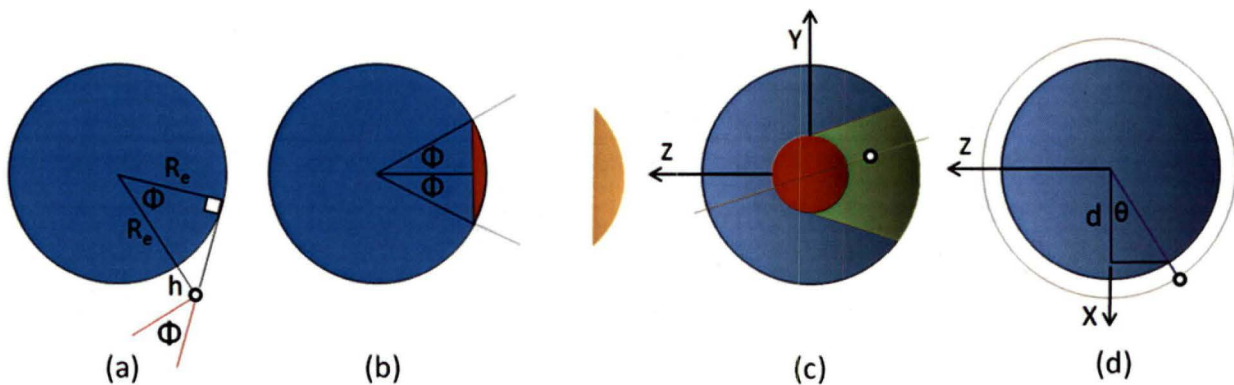


**Figure 8 – Relevant geometry for door control algorithm.**

When the satellite is orbiting the earth there is a zone (red circle, Fig. 8 c) directly in the center of the projected disk of the earth in which the door on the opposite-facing side of the experiment U can be opened without exposing the tank directly to earth IR. The diameter of this circle can be determined from Fig. 8 (a) and Equation 1.

$$\Phi = \arccos\left(\frac{R_e}{R_e + h}\right) \quad \text{Equation 1}$$

$2\Phi$  is the angle of a right circular cone (Fig. 8 b) originating at the center of the earth and intersecting the surface, creating a section which is the red circle projected in Fig. 16 c.

Due to the layout of the radiation shields on the craft relative to the actuating doors, there is an additional zone in which a door is free open to deep space. This zone is shown in shaded green in Fig. 8 c. The shape of this zone is due to the fact that as the satellite orbits earth, the relevant radius of the earth (line “d” in Fig. 8 d) grows smaller as  $\theta$  increases. Effectively, the earth is curving out of the view of the tank, widening the angle at which the door may be open. This can be seen by modifying Eq. 1 to replace one instance of  $R_e$  with  $d = R_e \cos(\theta)$ :

$$\Phi_{new} = \arccos\left(\frac{R_e \cos(\theta)}{R_e + h}\right) \quad \text{Equation 2}$$

This scheme is limited by some simplifying assumptions. While the analysis above does assume a simple square shape for the satellite experiment U, it otherwise treats the satellite as a point and therefore does not consider the specific geometry in more detail. Hence, there may be occasions when the satellite is in a “safe” zone but the disk of the earth may still be seen from the tank. Further, while the MLI earth shield is highly specular, it does have some diffusive reflection. This allows some earth IR to reach the tank by reflecting off the earth shield even if the earth is totally out of view.

### BASELINE THERMAL PERFORMANCE

The thermal model was run in the target orbit provided by the launch service organization. The thermal modeling of the spacecraft assumes the craft has been properly deployed from the PPOD (Poly Picosatellite Orbital Deployer) and the solar panels and radiation shields have deployed. It also assumes that attitude control and other onboard systems are functioning nominally. The orbit environment is determined by the variables listed in Table 1.

All components are initialized at 293K and allowed to cool asymptotically until the rate of further cooling is negligible. The time period required for this to happen was determined by experiment to be approximately 1.2e6 seconds (~14 days). As this point, the temperature is pseudo-steady state with the only changes caused by the regular door opening and closing procedure at various points in the orbit.

**Table 1 – Orbital Environmental Variables**

Planet Radius [km]	6378.14
Gravitational Mass [km <sup>3</sup> /s <sup>2</sup> ]	389601



Inclination of Equator [degrees]	23.44
Sidereal Period [s]	86164.1
Mean Solar Day [s]	86400
Solar Flux [W/m <sup>2</sup> ]	1354
Earth Albedo	0.35
IR Planetshine [K]	250

The final temperatures at the end of the transient analysis are shown in Figure 9. The mean temperature on the tank is 112.7K. The temperatures on the MLI radiation heat shield are non-physical, as these materials are modeled as arithmetic nodes with no thermal mass and can therefore change temperature instantaneously.

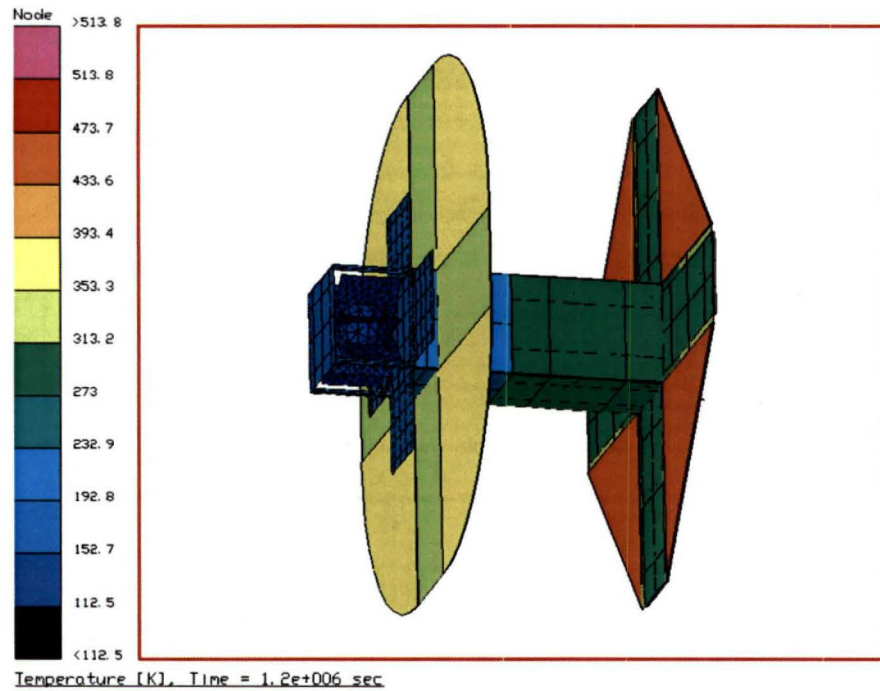


**Figure 9 – Temperature map of CC-1 after cooling.**

### PARAMETRIC ANALYSIS

Due to the passive cooling employed by CC-1 to reach cryogenic temperatures, the optical properties of various surfaces are very important. Several different materials and surface treatments were compared to find those with the best performance. Once determined, the properties of these materials were parameterized so that they could be degraded and the effect on

tank temperature determined. The most important optical surfaces are characterized by the MLI or the two coatings, listed in Tables 2 and 3 respectively.

**Table 2 – MLI Specifications**

MLI Specification	e* Value
MLI01	0.01
MLI03	0.03

**Table 3 – Coating Specifications**

Material	Solar Absorptivity	IR Emissivity
Silver coated Teflon	0.05	0.68
Z93SC55 coating	0.14	0.94

These materials and coatings are used throughout CC-1, with some of the components shown in Figure 10.

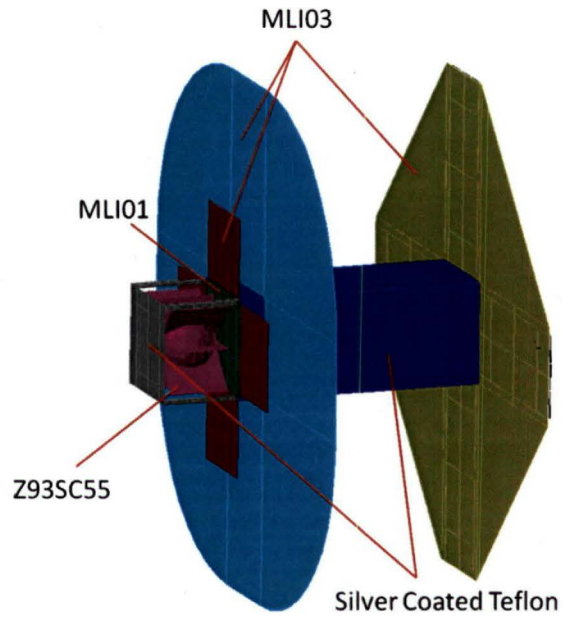


**Figure 10 – Optical materials use on CC-1.**

The optical properties of the materials were altered by various percentages to simulate degradation, environmental effects, flawed application, or other causes that may reduce thermal performance. The definition of performance “reduction” is as follows: the effective emissivity of MLI materials was increased, while the solar absorptivity was increased and the emissivity decreased for the coatings. Transient analyses were run for the same timespan as the baseline case, and the final temperature of the tanks compared in Table 4.

Material	Reduction (%)	Temp. (K)	Temp. Increase (%)
Silver Coated Teflon	10	112.8	0.1
Silver Coated Teflon	25	113.4	0.6
Silver Coated Teflon	50	115.2	2.2
MLI 0.1	50	113.3	0.5
MLI 0.1	100	113.6	0.8
MLI 0.1	200	114.1	1.2
MLI 0.3	50	112.8	0.1
MLI 0.3	100	112.9	0.2
MLI 0.3	200	113	0.3
Z93SC55	10	113.8	1.0
Z93SC55	25	116	2.9
Z93SC55	50	121.2	7.5

The variations in temperature as a percent are plotted versus the performance reduction percentage in the following Figures 11-14.

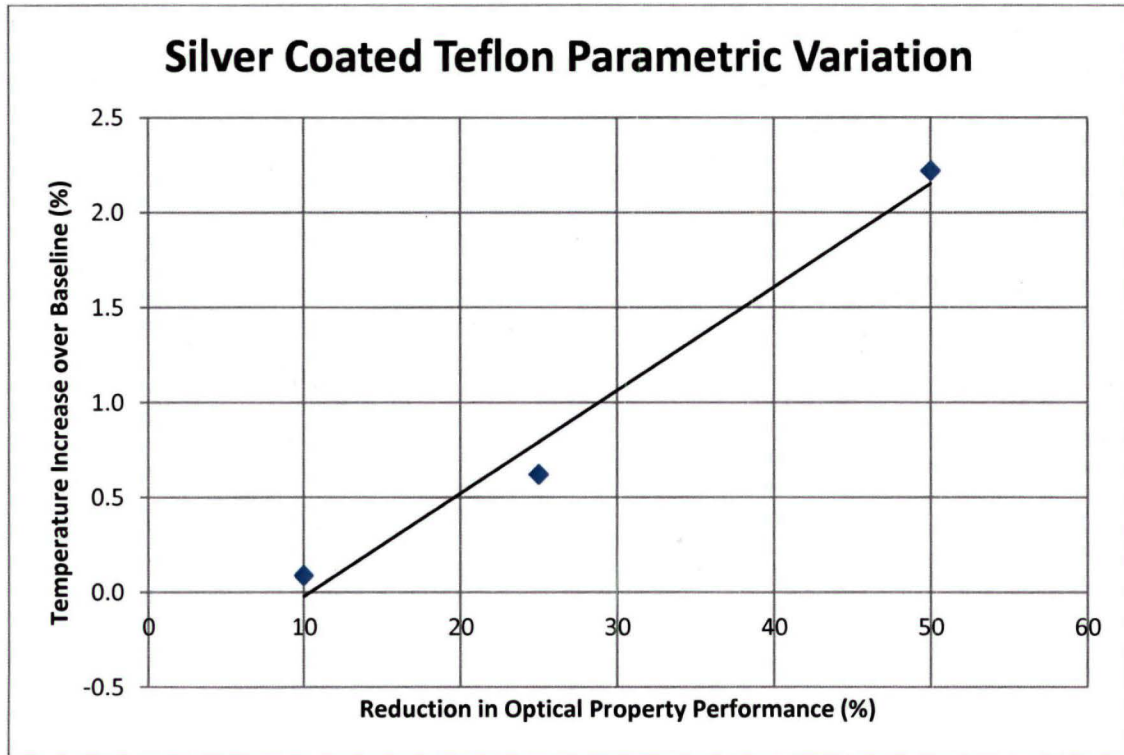


Figure 11

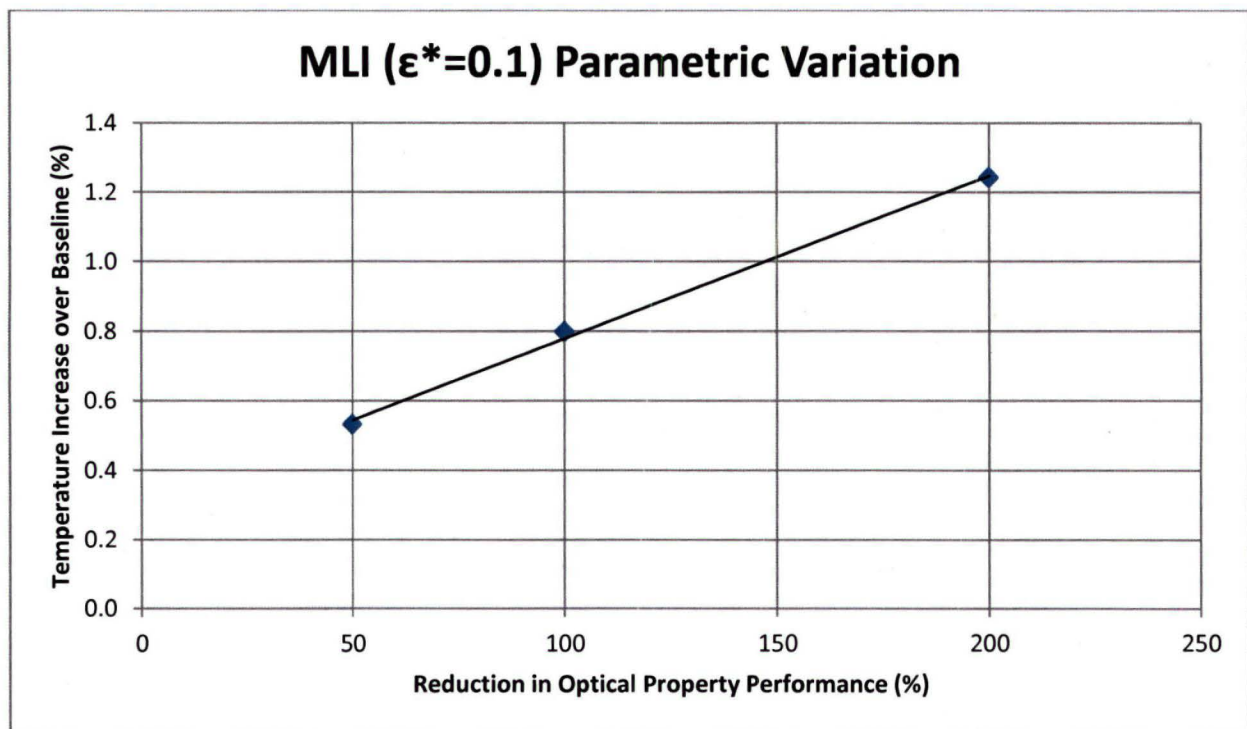


Figure 12

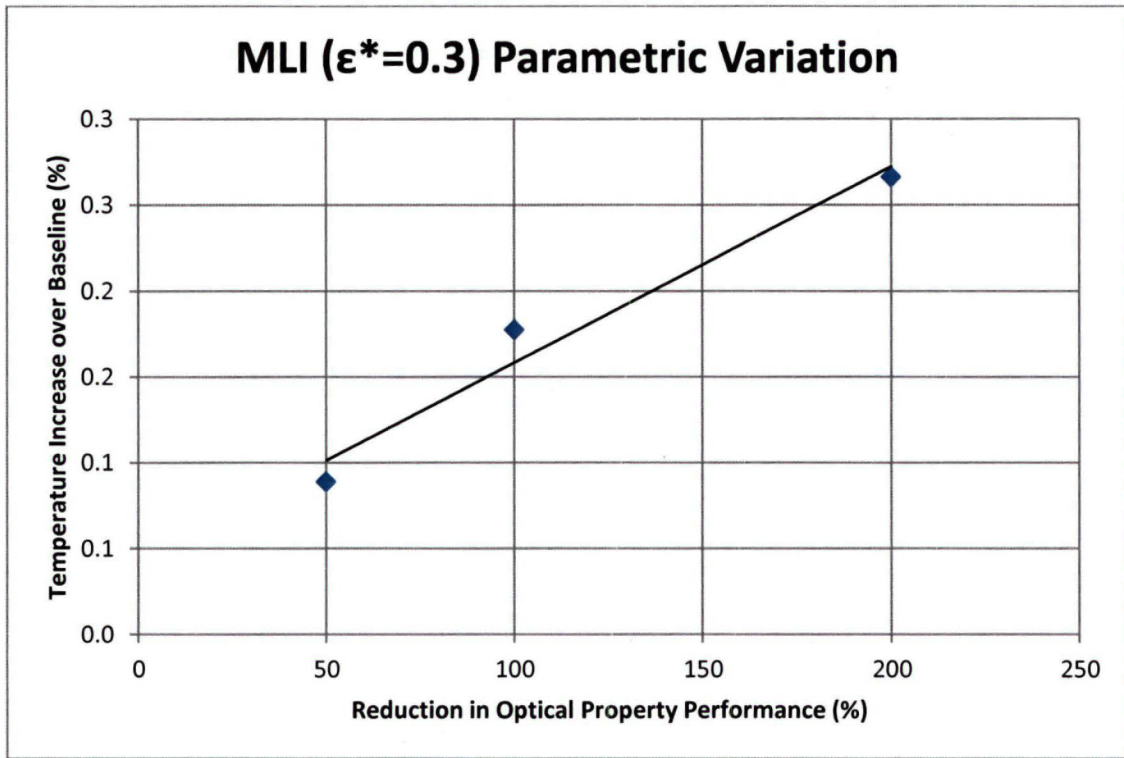


Figure 13

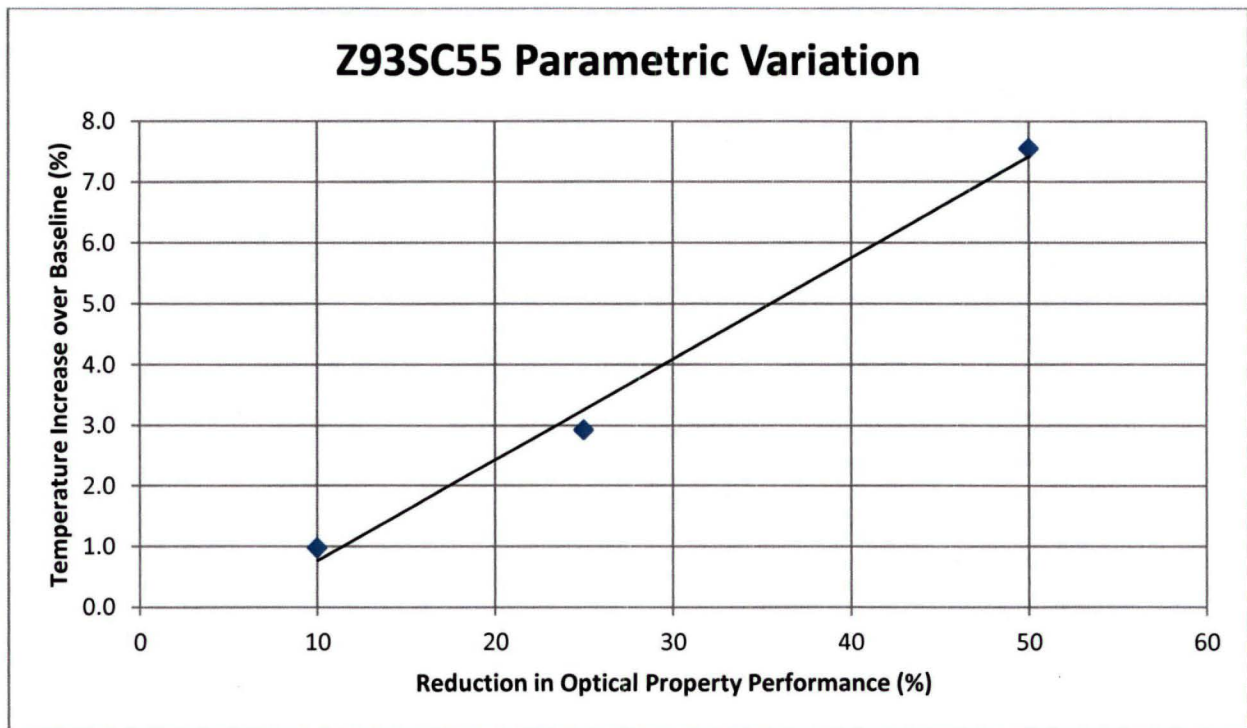


Figure 14

It is evident from these results that the thermal performance of CC-1 can sustain reductions in MLI performance quite well. The coatings are more important, with the most critical being the Z93SC55 applied to the experiment tank. Due to the low temperatures and limited surface area of the tank, it would be expected that this area would be most sensitive to changes in optical properties. Therefore, special attention must be paid to the application and protection of this coating before the spacecraft launch.

## **CONCLUSIONS**

This analysis demonstrates that the design concept for CC-1 is viable and will be able to produce cryogenic temperatures onboard. With an upper temperature limit of 120K, and a baseline temperature of 112.7 K resulting from analysis, an acceptable temperature margin exists for this stage of development. The model will be refined in the future with feedback from thermal vacuum tests and isolated hardware tests. The parametric analysis helped focus attention on which surfaces and coatings are most critical for adequate thermal performance. With continued effort, CC-1 will serve as a valuable technology demonstration for CFM technologies, and for cryogenic operations with the CubeSat platform.

## **NOMENCLATURE, ACRONYMS, ABBREVIATIONS**

e\* Effective Emissivity

IR Infrared

K Kelvin

Kg Kilogram

Km Kilometers

LEO Low Earth Orbit

M Meters

MLI Multi-Layer Insulation

MPa Megapascals

NASA National Aeronautics and Space Administration

PPOD Poly Picosatellite Orbital Deployer

S Seconds

U CubeSat Unit

W Watts

## REFERENCES

Meyer, M., Johnson, L., Palaszewski, Goebel, D., White, H., & Coote, D. (2012). *In-Space Propulsion Technology Roadmap*. Washington D.C.: National Aeronautics and Space Administration.